



An investigation in to the cascading effects on critical infrastructure by speeded up robust features in detection for landslides

Tim Chen^a, Tasawar, Hayat^b, Mourad Monsour^c, Emmanuel Anizoba Basorun^d, and John CY Chen^{e*}

^a Faculty of Information Technology, Ton Duc Thang University, Ho Chi Minh City, Vietnam
Email: timchen@tdtu.edu.vn

^b Quaid I Azam Univ 45320, Dept Math, Islamabad 44000, Pakistan

^c National University of Zimbabwe, Dept Hospitality Industry, Harare, Zimbabwe

^d Department of Urban & Regional Planning, University of Nigeria, Nsukka

^e BRAC Univ, Department of Tourism and Leisure, Dhaka, Bangladesh

Corresponding author*: jc343965@gmail.com

Abstract

Most of the frameworks in this field are limited by their capabilities. In this article, an insightful inspection framework for crash help and management is presented. The ideal management, necessities and upcoming program ideas have been pointed out. This has prompted a framework to be fundamentally dependent on ecological inspections in order to provide quotations and safety management to achieve autonomy in indigenous habitats. In this sense, ecological recognition is considered to be the place for the combination of slope data and the high level of diversity. Highlights of the findings are shown in the highlighted guide, and the focus of the coordinated discovery and coordination components is checked by distinguishing between highlights and element coordination. The diversity is effectively identified using both systems.

Keywords: cascading effects, critical infrastructure, detection, landslides, speeded up robust features.

Introduction

In recent years, global environmental changes have become increasingly prominent. This has led to an increase in the incidence of events and an increase in the outcome of various catastrophic events, such as earthquake tremors, tidal waves and avalanches caused by extreme storms, all of which greatly impact tourism and daily life in general. The catastrophic events have led to the impact of society, leading to the destruction of structures and harvests by disaster bases, causing enormous financial difficulties and even loss of personnel. Van Aalst (2006) describes the variables that influence atmospheric changes and the links between environmental changes and the atrocious climate 'miracles'. This information can be used to reduce the risk of catastrophic events. Of particular importance is the development of national procedures to develop and implement counter-productive effects and mitigate the effects of catastrophic events (Alcántara-Ayala, 2002). In general, the requirements of the catastrophic risk assessment, disaster location and design crash warning framework have proven to be indispensable in the near future. Work is currently underway to explore disaster assessment procedures to examine hazards from catastrophic events and to propose models for studying hazards (see, for example, Douglas (2007), Erdik et al. (2003), Lin et al. (2013a), Lin et al. (2013b), Jaffe and Gelfenbaum (2002), Luger et al. (2010), Huynh et al. (2017), Yu et al.'s other research focuses on the construction of natural disaster detection and early warning systems (Wu and Teng, 2002).

A number of strategies have been employed to study the extent of damage that can be caused by avalanche events and the parts that make up an avalanche. In contrast to traditional strategies, in this survey, we established a flotsam and jetsam warning framework that takes advantage of component-based PC vision methods. Component-based technology is reproducible, unique, and



robust, overcoming stimuli such as enlightenment changes and finding stable elemental focus, such as corners and edges of projects. Based on the true avalanche data captured by various gadgets, the adequacy of the strategy was examined in replication. In addition, a warning framework for avalanche occasions has been proposed. The rest of this article was organized as a task. First, the authoring work is discussed by exchanging the proposed framework's engineering and its modules. Next, the avalanche recognition strategy is used with the real case model and illustrates the usefulness of the avalanche occasion warning framework. Finally, we introduced our decisions and the potential outcomes of our future work.

Related Works

Catastrophic events can be divided into four categories, depending on terrain, climate, nature and the universe. In Taiwan, the most catastrophic events are earthquakes, tides and avalanches, which are representative of land and atmospheric disasters. Various studies of earthquake tremors have been completed in recent decades. Nakamura (1988) constructed the UrEDAS earthquake warning system, which consists of two steps: quick warning and precise warning. A brisk warning is given after the P wave has landed and an accurate warning is given after entering the S wave. Allen and Kanamori (2003) proposed an earthquake warning framework (Elarms) that uses the reappearance of arriving P waves to determine the degree of tremor and uses this data to warn that ground motion is being compromised. Wu and Zhao (2006) used P-wave sufficiency to assess the degree of tremor in early warnings.

Then, Nakamura (1988), Allen and Kanamori (2003), Wu and Zhao (2006) used remotely detected satellite telematics to distinguish the hazards of tremor. They found that by integrating optical information and some SAR highlights, the program of damage order can be completely improved. Others studied the tides and found interesting results. For example, Okal et al. (1999) studied Height measurements using satellite capture to determine the severity of the wave. They talked about seven cases, of which only two cases came into effect as a result of the Kuroshio. Greidanus et al. (2005) used a medium (25 m) target satellite radar symbol to identify damage from the torrent. Their approach is valuable for distinguishing beachside hazards. In different inspections of avalanche identification, Arattano and Marchi (2008) formed an avalanche observation and warning framework that included an advance guidance frame and a warning frame that was arranged using ultrasonic sensors. Jin and Xu (2011) used high-recursive radar to identify subsurface water content, which may trigger avalanches. Ellingwood (2001) used FORMOSAT-2 and HJ-1-B (environment and natural gas) to perform a general inspection of avalanches and Evaluation. Disaster Monitoring Constellation 1) Satellite, alone. Remote sensors are another gadget that can be used to identify catastrophic events.

Li et al. (2010) also uses wireless sensors, including COORDINATOR sensors and INSIDER sensors. The INSIDER sensor is used to collect landslide data, and the COORDINATOR sensor is a receiver that receives information from the INSIDER sensor. Lin et al. (2013a) Using a dual camera to build an extensive high-target inspection framework, you can observe item-by-item data. Strategies have been proposed to address catastrophic event identification issues and to develop a notification framework for catastrophic events. A variety of damage can be identified using similar gadgets. For example, it is undisputed that high-target satellite symbols can be used to investigate injuries and can also be used to identify tremors. Despite this, there is no mixing. Therefore, we propose a novel PC vision method that is based on prominence and can be used for the location of catastrophic events and accepts, for example, avalanches.

System Architecture

The proposed framework as figure 1 plans to distinguish avalanches and caution of the peril. So as to build an occasion cautioning framework, a few imperative assignments must be considered.

Firstly, we determine the atmospheric light for an input hazy UAVRS image.

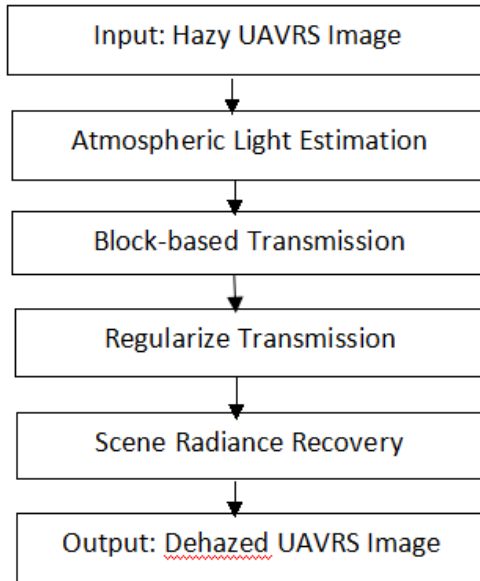


Figure.1: Block diagram of the UAVRS image dehazing algorithm

Background module

The background module aims to build stable feature points for the monitored scene before the occurrence of a landslide which can then be used to detect the variation in the environment. In this study, we used the SURF (Speeded up Robust Features) mechanism designed by Bay et al. (2006) to detect the feature points in the background and monitoring modules. This mechanism has the advantages characteristic of SURF which are repeatability, distinctiveness and robustness. In the SURF mechanism, the Hessian matrix is used for feature detection and is scaled to achieve the characteristic of scale invariance as shown in the following equation:

$$H(I, \sigma) = \begin{bmatrix} L_{xx} & L_{xy} \\ L_{xy} & L_{yy} \end{bmatrix}, \quad (1)$$

where $I=(x,y)$ is the image, σ is the scale which is the standard Gaussian deviation, and $L_{xx}(x, \sigma)$ is the Gaussian second order derivative at point x . The expression of $L_{xx}(x, \sigma)$ is shown as follows:

$$L_{xx}(I, \sigma) = G(\sigma) * I(x,y) \quad (2)$$

where $G(\sigma)$ is a Gaussian kernel function and $g(\sigma)$ is a Gaussian distribution function. The other symbols, $L_{xx}(I, \sigma)$ and $L_{yy}(I, \sigma)$, are similar to $L_{xx}(x, \sigma)$. The interesting features are selected from an image and are scaled according to the determinant of the Hessian matrix as shown in the following equation:

$$\det(H) = L_{xx}L_{yy} - (L_{xy})^2. \quad (3)$$

Bay et al. (2006) used the difference of Gaussian (DoG) to approximate the Laplacian of the Gaussian (LoG) and this is used with the integral images to reduce the computational cost. Therefore, the determinant of the Hessian matrix can be rewritten by using the following equation:

$$\det(H_{approx}) = D_{xx}D_{yy} - (\omega D_{xy})^2, \quad (4)$$

where ω is a parameter used to verify the errors cause by the DoG which is used to approximate LoG. Each feature is described as a vector of 64 dimensions including the orientation assignment

and the descriptor components. Finally, the robust feature points are detected from the different scales of the image.

In the background module procedure, the average number of detected features and the average number of matched features is evaluated at the same time. The percentage of variation in the features for both feature detection and feature matching is calculated as follows:

$$P_{fd_i} = \frac{N_{fd_i}}{Avg_{fd}} \quad \text{and} \quad P_{fm_i} = \frac{N_{fm_i}}{Avg_{fm}}, \quad (5)$$

where P_{fd_i} and P_{fm_i} are the percentage of variation of features in feature detection and feature matching at time i , respectively; N_{fd_i} and N_{fm_i} are the number of detected feature points and matched feature points, respectively; and Avg_{fd} and Avg_{fm} are the average number of detected features and matched features, respectively, calculated in the background module procedure.

Monitoring module

The authors estimate that atmospheric light A is the developed CI. In the work presented in this paper, the resilience framework was applied for urban flooding. To this purpose it was combined with fast flood modelling to evaluate possible flood scenarios, with the active participation of local authorities providing the scenarios. Thus, vulnerable CIs were identified, as well as the consequential flood. High visualization techniques were used to facilitate the understanding and communication of the results, while the outcomes were used for selecting suitable adaptation measures by local stakeholders. The whole approach and methodology have been applied to the Case Study of Torbay in South West UK and are presented in this paper. Finally, in the final selection of the region, we choose the color vector that minimizes the distance. By estimating the atmospheric and medium transmittance maps of the first two regions, we can recover the scene radiation image from the atmospheric scattering model.

Experimental results and discussion

We mainly evaluated the defogging effect through subjective observation. Figure 4 shows the dehazing image obtained by the method of He et al. and our improved approach. It can be seen from the observation that the dehazing effect of He is prone to chromatic aberration. The defogging (b) in the upper left corner of Figure 4 is blue, and the color of the whole image is blue, which is underestimated by the image. A partial image block of a brighter area.

No chromatic aberration is produced in this paper, and the defogging effect is more thorough and the image is clearer. 4(e) is an enlarged image of a red square area in the image of FIG. 4(d), and FIG. 4(c) is a fog-free image restored by the original article. Obviously, the details of the objects in this paper are clearer, the recovery of the White House area is significantly improved, and there are no artifacts around the object, mainly due to our correct prediction of atmospheric light values. And the regularization optimization of the dielectric transmittance map, we refer to the gradient information of the dehaze UAVRS image. Figure 5 shows some real UAVRS images. The fog-free image is more thoroughly defogged and has vivid colors, which fully demonstrates the superiority of our algorithm.

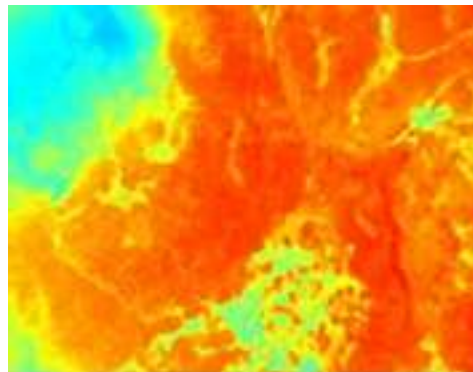
Conclusion

In this paper, we propose a dark channel-based dehazing model, and then defog the remote sensing image of the drone. The quadtree search method is used to find the best atmospheric light prediction position, thereby reducing the color distortion of the recovered fog-free image. In

addition, we propose a new regularization optimization scheme to smooth the dielectric transmittance map. The experimental results show that our dehazing algorithm can effectively recover clear UAVRS images. Such innovations help tourism site plotting for developments for example as the presence of haze in the atmosphere reduces the quality of images taken by visible camera sensors.



Figure.2: The results of feature-point matching in the simulation environment.



(a)

(b)

Figure.3: Transmission Estimation, (a)Haze UAVRS image, (b)He et al.'s refined transmission map, (c)our refined transmission map.



Figure.4: comparison of dehaze methods for UAVRS images.



Figure. 5: dehazing UAVRS image, (a)Haze UAVRS image, (b) He et al.'s results, (c) our results.

References

- Ahmed, O. S., Shemrock, A. & Chabot, D. (2017). Hierarchical land cover and vegetation classification using multispectral data acquired from an unmanned aerial vehicle. *International Journal of Remote Sensing*, 38(8) 2037-2052.
- Alcántara-Ayala, I. (2002). Geomorphology, natural hazards, vulnerability and prevention of natural disasters in developing countries, *Geomorphology*, 47(2), 107-124.
- Allen, R. & Kanamori, H. (2003). The potential for earthquake early warning in southern California, *Science*, 300, 786– 789.
- Arattano, M. & Marchi, L. (2005). Measurement of debris flow velocity through cross-correlation of instrumentation data, *Natural Hazards and Earth System Sciences*, 5, 137–142.
- Bay, H., Tuytelaars, T. & Van Gool, L.J. (2006). SURF: Speeded Up Robust Features, ECCV06 pp. 404-417
- Ellingwood, B. R. (2001). Earthquake risk assessment of building structures, *Reliability Engineering & System Safety*, 74(3), 251-262.
- Erdik, M., Aydinoglu, N., Fahjan, Y., Sesetyan, K., Demircioglu, M. & Siyahi, B., et al. (2003). Earthquake risk assessment for Istanbul metropolitan area, *Earthquake Engineering and Engineering Vibration*, 2(1), 1-23.
- Erdik, M., Şeşetyan, K., Demircioğlu, M.B., Hancılar, U. & Zülfiyar.C. (2011). Rapid earthquake loss assessment after damaging earthquakes. *Soil Dynamics and Earthquake Engineering*, 31(2), 247–266.
- Greidanus, H., Alvarez, M., Santamaria,C., Thoorens, F-X., Kourti, N. & Argentieri, P. (2017). The SUMO Ship Detector Algorithm for Satellite Radar Images, *Remote Sens.*, 9(3), 246; Available online at <https://doi.org/10.3390/rs9030246>



Hong, Yu., Hong P. Zhu., Shun Weng, Fei Gao., Hui Luo. & De M. Ai. (2018). Damage detection of subway tunnel lining through statistical pattern recognition, *Structural Monitoring and Maintenance*, 5(2), 231-242.

Huynh, T.C. et al. (2017). Advances and challenges in impedance-based structural health monitoring. *Structural Monitoring and Maintenance*, 4(4), 301.

Jaffe, B.E. & Gelfenbaum, G. (2002). Using tsunami deposits to improve assessment of tsunami risk. *Solutions to Coastal Disasters*, 2, 836-847.

Li, H.I., Yu, Y. & Ou, J.P. (2010). Design, calibration and application of wireless sensors for structural global and local monitoring of civil infrastructures. *Smart Struct Syst.*, 6(5-6), 641-659.

Lin, C.W., Hung, Y.P., Hsu, W.K., Chiang, L. & Chen, T. (2013a). The construction of a high-resolution visual resolution monitoring for hazard analysis, *Nat. Hazards*, 65(3), 1285-1292.

Lin, C.W., Chen, Hsu, W.K., Y., Tsai, H., Hung, Y.P. & Chiang, L. (2013b). Application of a feature-based approach to debris flow detection by numerical simulation, *Nat. Hazards*, 67(2), 1-14.

Lugeri, N., Kundzewicz, Z., Genovese, E., Hochrainer, S. & Radziejewski, M. (2010). River flood risk and adaptation in Europe-assessment of the present status, *Mitigation and Adaptation Strategies for Global Change*, 15(7), 621-639.

Nakamura, Y. (1988). On the urgent earthquake detection and alarm system (UrEDAS), paper presented at 9th World Conference on Earthquake Engineering, *Jpn. Assoc. for Earthquake Disaster Prev.*, Tokyo-Kyoto.

Radziejewski, M. (2010), River flood risk and adaptation in Europe assessment of the present status, *Mitigation and Adaptation Strategies for Global Change*, 15(7), 621 -639.

Thanh-Canh Huynh, Ngoc-Loi Dang & Jeong-Tae Kim. (2017). Advances and challenges in impedance-based structural health monitoring, *Structural Monitoring and Maintenance*, 4(4), 301-329.

van Aalst, M. (2006). The Impacts of Climate Change on the Risk of Natural Disasters, *Disasters* 30(1), 5-18 DOI: 10.1111/j.1467-9523.2006.00303.x

Vehbi; B. O. & Hoskara, S. O. (2009). A model of measuring the sustainability level of historic urban quarters. *European Planning Studies*, 17 (5), 715 -739.

Wu, Y.M. & Teng, T.U, (2002). A virtual subnetwork approach to earthquake early warning, *Bul. Seismol. Soc. Am.*, 92(5).

Zhu, Q., Mai, J. & Shao, L. (2015). A Fast Single Image Haze Removal Algorithm Using Color Attenuation Prior, *IEEE Transactions on Image Processing*, 24(11), 3522-3533.